Catena 206 (2021) 105561

Contents lists available at ScienceDirect

Catena

journal homepage: www.elsevier.com/locate/catena

Evolution of soil salinization under the background of landscape patterns in the irrigated northern slopes of Tianshan Mountains, Xinjiang, China

Qingwei Zhuang [a], Zhenfeng Shao [a,*], Xiao Huang [c], Ya Zhang [a], Wenfu Wu [b], Xiaoxiao Feng [a], Xianwei Lv [a], Qing Ding [a], Bowen Cai [b], Orhan Altan [d]

[a] State Key Laboratory of Information Engineering in Surveying, Mapping and Remote Sensing, Wuhan University, Wuhan 430079, China
[b] School of Remote Sensing and Information Engineering, Wuhan University, Wuhan 430079, China
[c] Department of Geosciences, University of Arkansas, Fayetteville, AR 72701, USA
[d] Department of Geomatics Engineering, Istanbul Technical University, Istanbul 36626, Turkey

ARTICLE INFO

Keywords:
Soil salinization
Landscape patterns
Cultivated land
Transfer matrix
Arid regions

ABSTRACT

Soil salinization has been a topic due to the widespread recognition of the food crisis and the shortage of cultivated land resources in arid regions. Unfortunately, the evolution of soil salinization under the background of landscape dynamics is rarely addressed due to the lack of spatial coupling techniques. Recent developments in soil science and remote sensing technology provide the possibility for accurate management of land resources. This study aims to explore the spatiotemporal variations of soil salinization by coupling the spatial distribution of soil salinization and landscape patterns in the irrigated northern slopes of Tianshan Mountains. We graded soil salinization levels based on analytic hierarchy process (AHP) method. The results indicated that the proportion of salinized cultivated land in 2014 (32.11%) was higher than that in 2005 (28.11%). We argue that simply quantifying the changes of soil salinization can neither accurately reflect the effectiveness of salinized cultivated land management nor meet the need for land resource planning. In response to these shortcomings, the evolution of soil salinization was explored in three categories, i.e., "stable cultivated land", "increased cultivated land", and "decreased cultivated land". We found that the proportion of soil salinization in stable cultivated land has dropped considerably from 38.11% in 2005 to 29.22% in 2014. This number in the increased cultivated land (59.11%) is much higher than that of the whole study area. These results are expected to benefit local authorities and assist in alleviating the food crisis in arid regions.

1. Introduction

Soil salinization refers to the salinity of the bottom soil or groundwater rises to the surface with capillary water (Nativ et al., 1997; Druhan et al., 2008; Xiao et al., 2019). After the evaporation process, the salt accumulates in the surface soil. Soil salinization is regarded as a combined effect of human factors and natural factors on the earth system, threatening nearly 20% of irrigated agriculture in the world (Adejumobi et al., 2016). It is worse in arid regions where 30% of the irrigated agriculture is in saline (Li et al., 2014), leading to declined crop productivity, land degradation, and reduced biodiversity (Daliakopoulos et al., 2016; Yang et al., 2019). To make things worse, the world is on the verge of the worst food crisis in at least 50 years (Asiedu et al., 2020). Nearly 690 million people suffered from hunger in 2019, an increase of 10 million compared with 2018 and an increase of nearly 60 million compared with 2014 (FAO, 2020). Kansiime et al. (2021) estimated that the number of chronically hungry people might increase by more than 130 million due to the Coronavirus Disease 2019 (COVID-19) and African locust plague at the end of 2020. In the context of a potential global food crisis, the evolution of soil salinization (referring to the range of cultivated land in this study) is important to the sustainable development of the irrigated agriculture and food security in arid regions.

For several decades, many efforts have been made to properly evaluate soil salinization (Shao et al., 2019a). The development of soil salinization evaluation methods in existing literature can be divided into three main stages: 1) sample analysis method, 2) geophysical prospecting test method, and 3) remote sensing (RS) technology (Funakawa et al., 2000; Gebremeskel et al., 2018b; Li et al., 2018; Shao et al., 2019b). In this session, we focus on reviewing the works in the third stage, i.e., mapping soil salinization using RS techniques. Khan et al.

* Corresponding author.
E-mail address: shaozhenfeng@whu.edu.cn (Z. Shao).

https://doi.org/10.1016/j.catena.2021.105561
Received 23 February 2021; Received in revised form 17 June 2021; Accepted 21 June 2021
Available online 1 July 2021

(2005) monitored the irrigated saline soil in Faisalabad, Pakistan, using data from the Indian Remote Sensing Satellite (IRS-1B). The application of hyperspectral remote sensing images benefits the identification and analysis of surface minerals and vegetation in salinized areas. It promotes a more accurate assessment of soil salinization (Dehaan and Taylor, 2002). Microwave remote sensing based on the relationship between EC and soil salinity (Aly et al., 2007), is another effective means to evaluate soil salinization. In general, the advantage of remote sensing technology lies in the existence of valuable historical data formed during the long-term earth observation process, providing data support for the long-term, large-scale dynamic monitoring of soil salinization (Jiang and Shu, 2019; Shao et al., 2020a).

Detecting and simulating dynamics of the land system plays an important role in understanding the environmental effects of human activities (Lambin, 2006; Zhang et al., 2020; Shao et al., 2020b). After ending the Land-Use and Cover-Change Project (LUCC) in 2005, the International Geosphere-Biosphere Programme (IGBP) and the International Human Dimension Programme (IHDP) jointly launched the Global Land Project (GLP) in 2006 (IGBP, 2005). GLP, aiming to understand the human-environment coupling system, emphasizes comprehensive integration and simulation research of the human-environment coupling system in the global terrestrial system (Liu et al., 2020). Existing studies have shown that changes in landscape patterns are responsible for the heterogeneities in geophysics and geochemical cycles (Bordonal et al., 2017; Gao and O'Neill, 2020), and they can also lead to changes in soil properties and land productivity, thereby greatly affecting soil conditions (Wang et al., 2019). Soil salinization, as one of the important causes of cultivated land degradation, is also affected by the negative feedback of landscape pattern changes (e.g., unorganized urbanization) (Smith et al., 2016). Therefore, exploring the evolution characteristics of soil salinization under the background of landscape patterns is expected to facilitate the understanding of the pressure from human activities on cultivated land resources.

Arid regions, accounting for 41% of the world's land area, are home to 38% of the population in the world (Yaseen et al., 2020). Given their sensitivity to climate change, arid regions deserve more attention, as they tend to own the most fragile landscape ecosystem and the most serious soil salinization issues (Jiang et al., 2019; Zhuang et al., 2020). The huge population, coupled with the fragile ecosystem, creates severe soil salinization in the arid regions (Huq et al., 2019; Jordan et al., 2010). Existing studies are limited, as they tend to focus on the impact of landscape pattern dynamics from a certain soil factor. Although these studies explained the ecological and geochemical effects of land use changes (Bless et al., 2018; Islam et al., 2019; Lakhdar et al., 2009), few comprehensively evaluate the effects of soil salinization under the background of landscape patterns. To fill this gap, we aim to provide important scientific references to formulate land planning policies in arid regions.

In this study, the landscape patterns obtained by land satellite (Landsat) images were used for monitoring the dynamics of cultivated land. Taking the northern slope of Tianshan Mountains as the study region, we combined a large number of soil samples to identify the spatiotemporal characteristics of soil salinization. In this study, we aim to: (i) assess the level of soil salinization through a new regionally applicable method; (ii) explore the evolution characteristics of soil salinization from 2005 to 2014; (iii) investigate the impacts of landscape pattern changes on soil salinization; (iv) identify the effectiveness of soil salinization control and the sustainable development planning of oasis agriculture in arid regions.

2. Methods and material

2.1. Study area

The northern slope of Tianshan Mountains, located in the hinterland of the Eurasian continent, is a long and narrow area along the Tianshan Mountains at 42°50′N–46°12′N and 79°53′E–92°06′E (Fig. 1). It is about 14.66×10^4 km^2 in size, accounting for 8.78% of the area of the Xinjiang Province. The climatic features are characterized by cold and long in winter, hot and dry in summer, and large temperature differences between day and night. According to the statistics of the meteorological stations from 2005 to 2014 (http://data.cma.cn/), the average annual precipitation, mainly concentrated in May and June, is between 150.13 and 360.81 mm. Precipitation varies greatly in different sub-regions (richest in the west sub-district and lowest in the east sub-district). The average annual temperature is between 4.5 and 7.0 °C (highest in July at 23.7 °C, lowest in January at −10.4 °C).

As one of the huge mountain series in central Asia, the Tianshan Mountains span many countries. The northern slope of the Tianshan Mountains is mainly composed of Jurassic strata with its front mountains and low hills covered by loess. This has caused differences in the geographical location and natural conditions of the sub-areas. These sub-areas are under the jurisdiction of different administrative units. As a result, differences in policies, culture, and other directions have been caused, which show different patterns of land resource utilization. Some studies have been carried out on the eastern, central and western parts of the northern slope of Tianshan Mountain. This study can provide them with more data references. With the complex diversity of climate, geology, and geomorphology, the soil structure in the study region presents a vertical distribution pattern as a whole. Severe soil salinization occurs in the irrigated areas, posing a great threat to local food security. Meanwhile, rapid urbanization also endangers cultivated land. Given the above reasons, we decided to explore the evolution of soil salinization under the background of landscape patterns in this area.

2.2. Methods

The evaluating methodology of soil salinization under the background of landscape patterns was established (Fig. 2). Firstly, the Random Forest method is used to obtain land cover/land use data from Landsat images. This classification results passed the accuracy verification. Secondly, the collected soil data is tested in the laboratory. Thirdly, we used the Delphi method to select 6 out of 14 indicators that appeared in previous studies to evaluate soil salinization. Fourthly, we explored the spatiotemporal changes of landscape patterns and soil salinization during the study period. Finally, the evolution characteristics of soil salinization under the background of landscape patterns were explored via Transfer Matrix method.

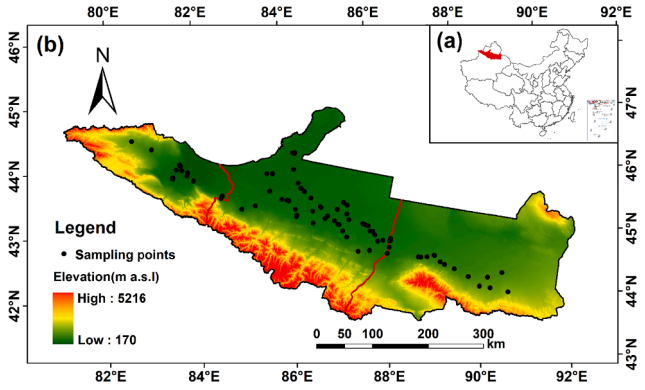

Fig. 1. (a) Location of the northern slope of Tianshan Mountains in China; (b) distribution of sampling points in study area (Boundary information was obtained from the Ministry of Natural Resources of China, Approve number: GS (2019)1682). The red lines represent the boundary line between the east, central, and west sub-district of the northern slope of the Tianshan Mountains. (For interpretation of the references to color in this figure legend, the reader is referred to the web version of this article.)

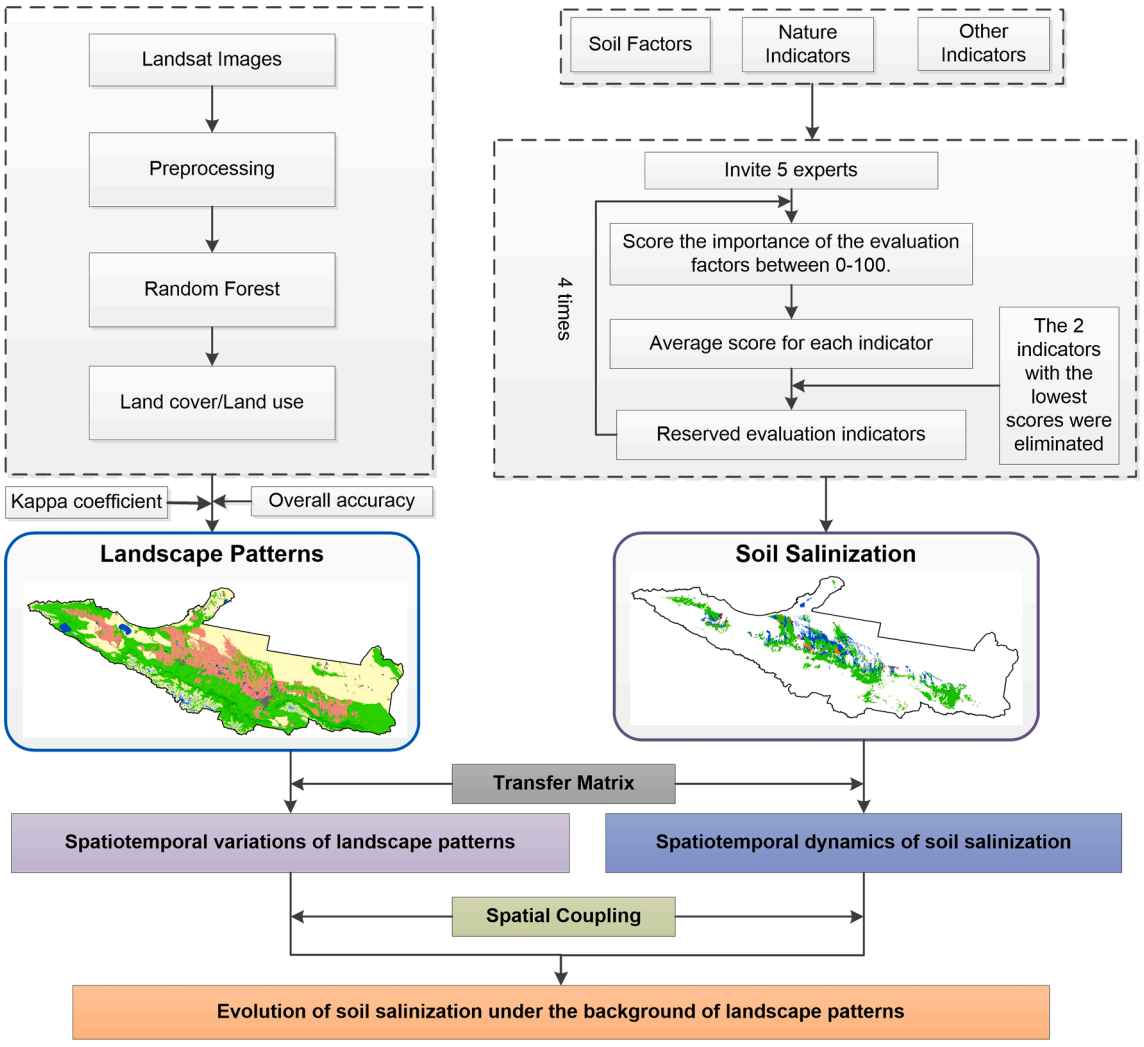

Fig. 2. Technological process for evaluating of soil salinization under the background of landscape patterns.

2.2.1. Soil samples

Soil samples were obtained in May 2005 and May 2014 (not-crop growth period). The specific spatial distribution of 73 sampling points (16 in the east sub-district, 44 in the central region, and 13 in the west sub-district) can be found in Fig. 1. The depth of the sampling points ranges from 20 cm to 30 cm. A total of five repetitive samplings were set at each sampling point. We avoided the sidewalks, ditches, and micro terrains during sampling. More details can be found in Fig. S1 and Fig. S2. Specifically, we conducted a parallel laboratory analysis on nine indicators, i.e., *total salt (TS)*,*pH*, Cl^-,SO_4^{2-}, Ca^{2+}, K^+, Mg^{2+}, Na^+, and HCO_3^-. The testing method and results are shown in Table S1.

2.2.2. Interpretation of landscape patterns

Six major landscape patterns (i.e., wood land, grass land, cultivated land, water body, construction land, and barren land) were extracted from Landsat images via the Random Forest method (Hoffman et al., 2018). The satellite images were captured on June 12, 2005 and August 31, 2014, with 18 sceneries in each phase. The classification accuracy was evaluated via overall accuracy and kappa coefficient. The overall accuracy, representing the probability that the classification result of each random sample is consistent with the actual value of the corresponding region, suggests the proportion of pixels that are correctly classified for LUCC categories (Bai et al., 2019). The kappa coefficient, considering both the correct and the incorrect pixels, was used to characterize the degree to which the two maps agreed (derived categories are consistent with Google Earth high-resolution images, field-measured data, or credible classifications). A kappa coefficient greater than 0.75 generally indicates a good agreement between the two images (Tang et al., 2015). A total of 134 random points were generated on both Landsat images and reference data to evaluate the classification accuracy. We found that the overall accuracy was 92.00% in 2005 and 92.26% in 2014. The kappa coefficient was 0.89 in 2005 and 0.90 in 2014. Both overall accuracy and kappa coefficient indicated that the classification result was reliable.

2.2.3. Mapping soil salinization

Based on the classification system of soil salinization in the second soil survey in Xinjiang, this study established an assessment method for soil salinization via the analytic hierarchy process (AHP) method in the irrigated northern slopes of Tianshan Mountains.

The selection of evaluation indicators is the most important step in the process of mapping the spatial distribution of soil salinization (Fig. S3). We selected 4 factors with the greatest impact on soil salinization, i.e., *TS, pH*,Cl^-, andSO_4^{2-}, using the principal component analysis (PCA) method (Table 1). We used the digital elevation model (DEM) and slope to express the natural conditions of cultivated land, given the fact that natural conditions of cultivated land also have a great influence on soil salinization. DEM and slope data were collected from the Resource Environmental Science and Data Center, Chinese Academy of Sciences (http://www.resdc.cn).

Table 1
Gradings of soil salinization classification indicators.

Guidelines	Indicators	Scoring standard					
		100	80	60	40	20	0
Soil conditions	TS (g/kg)	<3.5	3.5–5.0	5.0–6.0	6.0–8.5	8.5–10.0	>10.0
	pH	<8.5	8.5–9.0	9.0–9.5	9.5–10.0	10.0–10.5	>10.5
	Cl^- (g/kg)	<7.0	7.0–9.0	9.0–13.0	13.0–16.0	16.0–20.0	>20.0
	SO_4^{2-} (g/kg)	<8.0	8.0–10.0	10.0–15.0	15.0–20.0	20.0–25.0	>25.0
Natural indicators	DEM (m)	0–500	500–1000	1000–1500	1500–2000	2000–2500	>2500
	Slope (°)	<1.0	1.0–3.0	3.0–5.0	5.0–7.0	7.0–10.0	>10.0

Further, the ordinary kriging method was used to visualize the selected factors of 50 sampling points. We used the remaining 23 sampling points to verify the results of the spatial visualization. The Pearson correlation coefficients between the verified and simulated values of *TS, pH,* Cl^-, and SO_4^{2-} are 0.921, 0.873, 0.705, and 0.719, respectively, suggesting that the results of spatial visualization have high credibility (Fig. S3).

Finally, we obtained the score of soil salinization by aggregating the scores corresponding to each indicator:

$$score = \sum_{i=1}^{n} F_i \quad (1)$$

where F_i refers to the score of the *i-th* factor; n represents the number of factors. A higher score suggests cultivated land with lighter soil salinization. To better understand the distribution of soil salinization, we divided soil salinization into four levels according to the score. The specific grading standards are presented as follows: [0, 25] is defined as severe salinization; (25, 50] is defined as moderate salinization; (50, 75] is defined as mild salinization; (75, 100] is defined as none salinization.

2.2.4. Transfer matrix method

Proposed in the early 20-th century, the transfer matrix method assumes that certain factors of a system are in transition, and the n-th result is only affected by the (n-1)-th result (Hong et al., 1993; Kunst and Dwivedi, 2019). We believe that this approach can reflect the followingchanges: (1) area of salinized cultivated land at different grades in the two periods; (2) amount of salinized cultivated land at different grades from the previous period to the next period; (3) number of salinized cultivated land in the latter period was transferred from the previous period. The transfer matrix method is able to analyze the quantitative and structural characteristics of regional landscape changes and the specific directions of changes in various landscape patterns in a comprehensive manner. More details of the transfer matrix method can be found in Table S2.

3. Results

3.1. Distribution of soil salinization in cultivated land

3.1.1. Analysis of soil salinization in cultivated land in 2005

Based on the aforementioned assessment approach, we derived the spatial distribution of soil salinization in cultivated land in 2005. We observed that none salinization was dominant in the study area (15,399.87 km^2, occupying 71.19% of the total area of cultivated land) in 2005. However, nearly 30% of cultivated land was threatened by soil salinization, including mild salinization at 23.06%, moderate salinization at 5.14%, and severe salinization at 0.01%.

Affected by natural factors (e.g., precipitation, temperature, and soil conditions) and socio-economic factors (e.g., population, urbanization, and policy), the amount of cultivated land varies greatly in sub-districts: 6,086.33 km^2 in east sub-district, 12,772.53 km^2 in central sub-region, and 2,593.59 km^2 in west sub-district (Table 2). In the east sub-district, the areas of mild salinization, moderate salinization, and severe salinization were 980.80 km^2, 186.58 km^2, and 0.28 km^2, respectively. The central sub-region had the largest area of salinized cultivated land (4,120.75 km^2), occupying 32.26% of the total cultivated land. In this sub-region, mild salinization, moderate salinization, and severe salinization respectively cover 3,328.58 km^2, 791.01 km^2, and 0.28 km^2. In the west sub-district, salinized cultivated land accounted for 29.47% of the total cultivated land. No severe salinization occurred in the west sub-district.

Table 2
Area and proportion of soil salinization within different sub-districts in 2005.

Grade		Regions			
		Eastern	Central	Western	Total
None salinization	Area (km^2)	4918.67	8651.78	1829.42	15399.87
	Proportion (%)	80.82	67.74	70.53	71.79
Mild salinization	Area (km^2)	980.80	3328.58	638.51	4947.89
	Proportion (%)	16.11	26.06	24.62	23.06
Moderate salinization	Area (km^2)	186.58	791.01	125.66	1103.25
	Proportion (%)	3.07	6.19	4.85	5.14
Severe salinization	Area (km^2)	0.28	1.16	0.00	1.44
	Proportion (%)	0.00	0.01	0.00	0.01
Total	Area (km^2)	6086.33	12772.53	2593.59	21452.45
	Proportion (%)	28.37	59.54	12.09	100

The results pointed out the spatial homogeneity as well as heterogeneity in the distribution of soil salinization. In the study area and within each subdistrict, cultivated land with none salinization occupies was dominant, followed by mild salinization. While cultivated land with severe salinization covers the least areas. However, we observed that areas and proportions in cultivated lands with different salinization severity present different patterns within each subdistrict. Therefore, when formulating salinization treatment policies, it is necessary to consider the regional discrepancies.

3.1.2. Analysis of soil salinization in cultivated land in 2014

The distribution of soil salinization in 2014 was similar to that in 2005 (Fig. 3). None salinization was still dominant in study area (occupying 67.89%). Soil salinization was largely confined to the central sub-region (5,186.05 km^2, occupying 66.61% of the total area of soil salinization).

By comparing the two time periods, we find considerable differences in the quantity and composition structure of cultivated land. For example, the total area of cultivated land was increased by 2,794.11 km^2 (from 21,452.45 km^2 to 24,246.56 km^2). With the increased cultivated land, however, the amount and the proportion of salinized cultivated land have increased considerably (6079.62 km^2, occupying 28.34% in 2005; 7785.17 km^2, occupying 32.11% in 2014). We attempt to explore the reasons for this worrying phenomenon in Section 3.2 and Section 3.3.

In 2014, the proportion of cultivated lands with soil salinization was

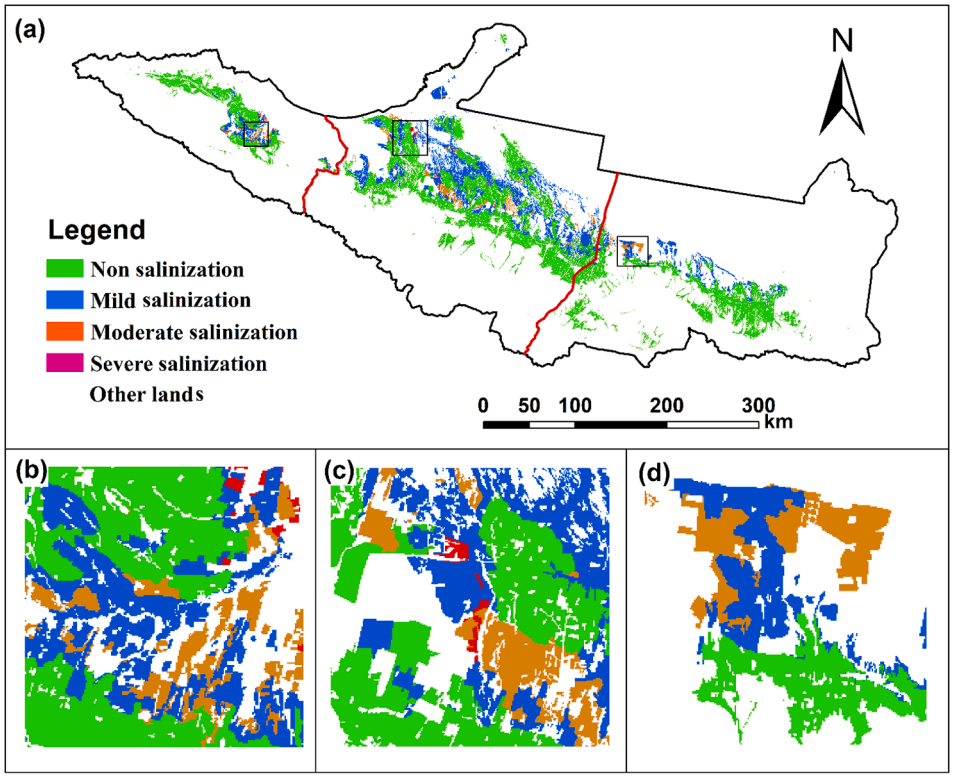

Fig. 3. **(a)** Distribution of soil salinization in cultivated land in 2014; soil salinization in the west **(b)**, central **(c)**, and east sub-district **(d).**

lowest in the east sub-district (1565.18 km^2, accounting for 25.28% of the area of cultivated land), including mild salinization with 1352.95 km^2 and moderate salinization with 212.23 km^2 (Table 3). Same as that in 2005, the proportion of salinized cultivated land was also the highest in the central sub-region (5186.05 km^2, occupying 35.45%), most of which were mild salinization (4695.62 km^2). In the west sub-district, the proportion of none salinization was less than 70%, indicating that the salinization problem is severer in this sub-district comparing to the overall situation of the study area.

The above results reflect only the distribution of soil salinization in terms of quantity, which is not sufficient to provide reasonable suggestions for the potential mitigation measures targeting the soil salinization problem. Therefore, we further discuss the spatiotemporal characteristics of soil salinization in the next sessions.

Table 3
Area and proportion of soil salinization within different sub-districts in 2014.

Grade		Regions			
		Eastern	Central	Western	Total
None salinization	Area (km^2)	4626.32	9443.79	2390.85	16460.96
	Proportion (%)	74.72	64.55	69.80	67.89
Mild salinization	Area (km^2)	1352.95	4395.62	834.64	6583.21
	Proportion (%)	21.85	30.05	24.37	27.15
Moderate salinization	Area (km^2)	212.23	789.37	199.23	1200.83
	Proportion (%)	3.43	5.39	5.82	4.95
Severe salinization	Area (km^2)	0.00	1.06	0.50	1.56
	Proportion (%)	0.00	0.01	0.01	0.01
Total	Area (km^2)	6191.50	14629.84	3425.22	24246.56
	Proportion (%)	24.55	62.54	12.91	100

3.2. Dynamics of soil salinization in cultivated lands from 2005 to 2014

We found observable transition among soil salinization of different levels from 2005 to 2014 after investigating the spatiotemporal map of soil salinization and interpreting the results from the transfer matrix. In terms of spatial distribution, there existed mutual transfer among different degrees of soil salinization in cultivated land and strong changes between cultivated land and other landscape patterns (Fig. 4).

We found that cultivated land with none salinization decreased by 485.73 km^2, most of which was converted to other land use types (472.79 km^2), a small amount was converted to mild (11.37 km^2) and moderate salinization (1.57 km^2) (Table 4). Newly identified none salinized cultivated lands cover 1546.82 km^2. 53.35 km^2 of mild soil salinization and 27.32 km^2 of moderate salinization were transformed into none salinization. Despite that the net increase in none salinization was 1061.09 km^2, a large amount of high-quality cultivated land was converted to other landscapes, mainly including construction land and grassland. The farmland abandonment resulting from urbanization deserves further attention.

Mild salinization was dominant in cultivated land (81.75% in 2005 and 84.56% in 2014). The net increase in mild salinization was 1575.32 km^2. 53.35 km^2 of mild salinization was converted to none salinization (53.35 km^2), and 246.01 km^2 was converted to other landscapes (246.01 km^2). Meanwhile, 82.70 km^2 of moderate salinization and 1857.51 km^2 of other landscapes were converted to mild salinization. Compared with none/mild salinization, cultivated lands with moderate and severe salinization pose great challenges in management and improvement. After the implementation of some mitigation measures, 27.32 km^2 of moderate salinization was converted into none salinization, and 82.70 km^2 was converted to mild salinization. Despite the promising results from these treatments, we observed that area of newly converted moderate salinization covers a considerably large space (244.49 km^2). Compared with other grades of soil salinization, the proportion of severe salinization was very low. Converting cultivated lands with severe salinization to woodland (e.g., Haloxylon

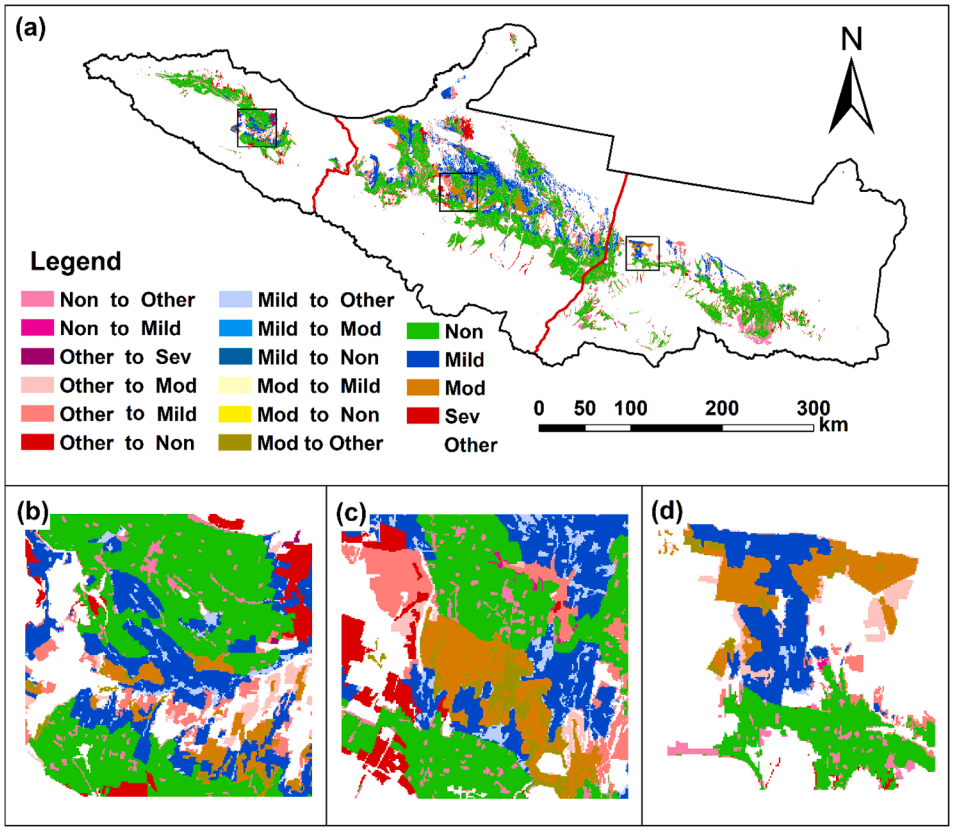

Fig. 4. **(a)** Spatial transformation map of soil salinization in cultivated land from 2005 to 2014; transformation details of soil salinization in the west **(b)**, central **(c)**, and east sub-district **(d)**. Note: Non, none salinization; Mild, mild salinization; Mod, moderate salinization; Sev, severe salinization.

Table 4
Transfer matrix of soil salinization in cultivated land from 2005 to 2014 (unit: km^2).

Year	Grade	2014						
		Non	Mild	Moderate	Severe	Other	Total	Decrease
2005	None	14914.14	11.37	1.57	0.00	472.79	15399.87	485.73
	Mild	53.35	4631.52	17.01	0.00	246.01	4947.89	316.37
	Moderate	27.32	82.70	956.34	0.55	36.34	1103.25	86.91
	Severe	0.00	0.11	0.32	1.01	0.00	1.44	0.43
	Other	1466.15	1857.51	225.59	0.00	121624.78	125174.03	3549.25
	Total	16460.96	6583.21	1200.83	1.56	122379.92	146626.48	\
	Increase	1546.82	1891.69	244.49	0.55	755.14	\	

ammodendron and Tamarix chinensis) can be a preferred option, given the low cost of such conversion.

3.3. The response of landscape pattern changes to soil salinization

3.3.1. Spatiotemporal variations of landscape patterns

Changes in landscape patterns can produce a series of physical and chemical effects. Fig. 5 presents the distribution, composition, and spatial dynamics of landscape patterns in the study area. Despite the notable discrepancies in landscape patterns in 2005 and 2014, their distribution was rather similar. Taking 2014 as an example, the main landscapes include grassland (60,326.92 km^2, occupying 41.14% of the study area), barren land (52,664.20 km^2, occupying 35.92%), and cultivated land (24,246.56 km^2, occupying 16.54%). The remaining three landscapes (including water bodies, construction land, and woodland) accounted for 6.40% of the study area. We observed that increased cultivated land is larger than the decreased cultivated land (Fig. 5).

The transfer matrix of landscapes was obtained by overlaying the landscape dataset from 2005 to 2014 (Table 5). The statistical results showed that the landscapes had undergone tremendous changes. The scales of conversion among various landscape patterns were notably different.

We noted two phenomena. First, cultivated land encroached a large amount of grassland (3187.66 km^2), accounting for 86.54% of the increased cultivated land. This phenomenon can be explained by the pressure of population and agricultural economy, which worried us as it may bring huge challenges to the water resources and environmental security in arid region. Second, cultivated land has decreased by 889.44 km^2, of which 604.79 km^2 was converted into construction land. Lost cultivated land were found concentrated around the urban fabrics, suggesting that the process of urbanization poses a serious threat to farmland and food security. The above results indicated that human activities play an important role that drives the changes in landscape patterns.

3.3.2. Comparative analysis of soil salinization in the conversion zones

To evaluate the changes and governance of soil salinization in

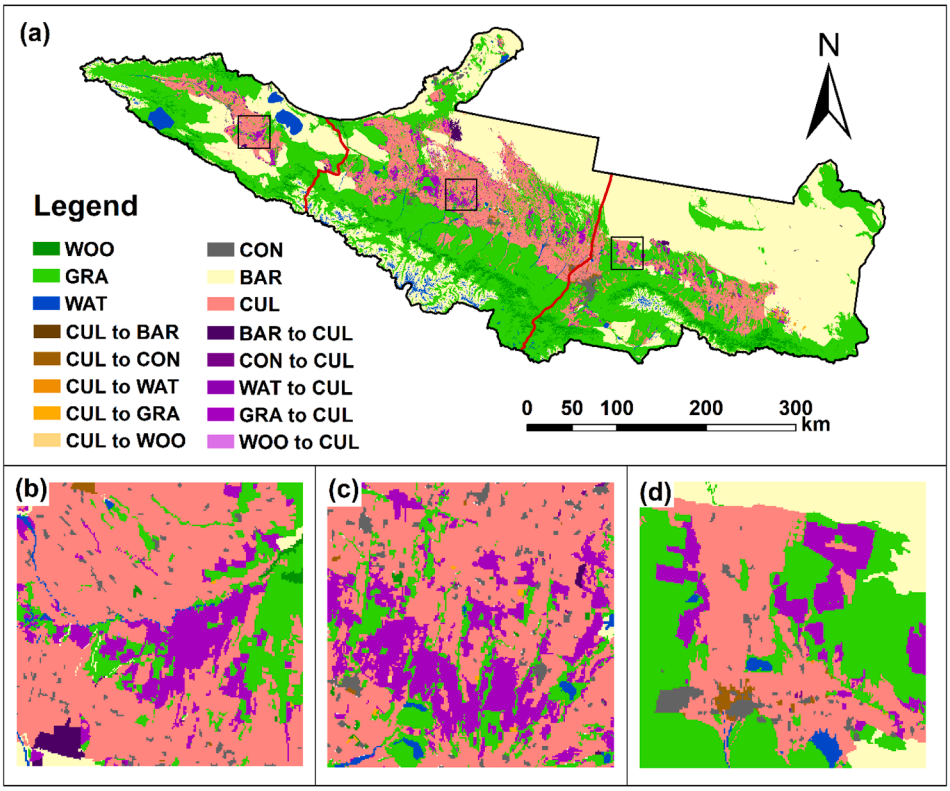

Fig. 5. **(a)** Dynamics of soil salinization in the study area from 2005 to 2014; soil salinization dynamics from 2005 to 2014 in the west **(b)**, central **(c)**, and east sub-district **(d)**. Note: WOO, woodland; GRA, grassland; WAT, water body; CON, construction land; BAR, barren land; CUL, cultivated land.

Table 5
Transfer matrix of landscape patterns between 2005 and 2014 (unit: km^2).

Year	Patterns	2014							
		WOO	GRA	WAT	CON	BAR	CUL	Total	Decrease
2005	WOO	3055.89	239.63	0.13	6.84	0.05	15.2	3317.74	261.85
	GRA	52.47	55831.41	135.47	501.05	1041.61	3187.66	60749.67	4918.26
	WAT	0.25	36.15	2803.96	5.75	162	4.83	3012.94	208.98
	CON	0.92	6.11	2.87	1912.89	0.89	22.56	1946.24	33.35
	BAR	5.41	3936.94	51.9	241.95	51457.94	453.3	56147.44	4689.5
	CUL	3.77	276.68	2.49	604.79	1.71	20563.01	21452.45	889.44
	Total	3118.71	60326.92	2996.82	3273.27	52664.2	24246.56	146626.48	\
	Increase	62.82	4495.51	192.86	1360.38	1206.26	3683.55	\	\

Note: WOO, woodland; GRA, grassland; WAT, water body; CON, construction land; BAR, barren land; CUL, cultivated land.

cultivated land in a more accurate manner, we divided cultivated land into three types: “decreased cultivated land”, “increased cultivated land”, and “stable cultivated land”. “Decreased cultivated land” refers to the cultivated land converted to other landscape types during the study period (e.g., from cultivated land to construction land). “Increased cultivated land” refers to the cultivated land converted from other landscape types (e.g., from grassland to cultivated land). “Stable cultivated land” refers to the cultivated land that has not been eroded by other landscape types.

The area of decreased cultivated land was 889.44 km^2, of which cultivated land with none, mild, and moderate soil salinization accounted for 86.05%, 8.72%, and 5.23%. Particularly, there were considerable differences in the composition and structure of cultivated land, which was converted into other landscapes. The areas, where cultivated land converted into woodland, barren land, and water bodies, were less than 10 km^2. Thus, they were not the focused analysis in this study (Pillar 1, 3, and 5 of Fig. 6). Cultivated land converted into construction land (604.79 km^2) consisted of 93.86% none salinization, 3.08% mild salinization, and 3.05% moderate salinization (Pillar 2 of Fig. 6). None salinization accounted for 73.73% of the cultivated land, which was converted into grassland (276.68 km^2) (Pillar 4 of Fig. 6). We also observed that a certain amount of salinized cultivated land has degraded into grassland (mild salinization accounted for 17.26%, moderate salinization accounted for 9.00%). The above results indicated that urbanization, coupled with the policy of “returning cultivated land to grassland or woodland”, is largely responsible for the decrease in cultivated land.

Compared with the decreased cultivated land, more increased cultivated land has been reclaimed by encroaching other landscapes (3683.55 km^2). The cultivated land encroached on water bodies, woodland, and construction land were rather trivial, and the converted cultivated land was dominant by none salinization (Pillar 7, 8, and 10 of Fig. 6). Among the cultivated land converted from barren land, none salinization accounted for more than three-quarters, and the rest was mainly categorized as mild salinization (22.23%) (Pillar 6 of Fig. 6).

The cultivated land converted from grassland was composed of soil salinization of various grades , nearly half of mild salinization (46.81%), a considerable amount of moderate (15.53%) and none salinization

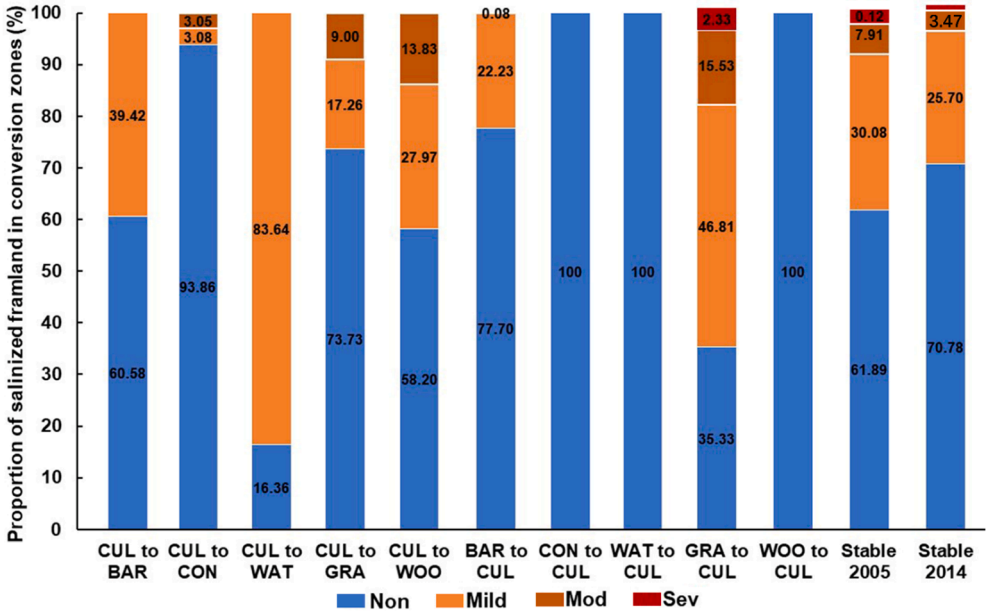

Fig. 6. Proportions of areas in four soil salinization categories (severe, moderate, mild, and none) in the decreased, increased, and stable cultivated land. Note: WOO, woodland; GRA, grassland; WAT, water body; CON, construction land; BAR, barren land; CUL, cultivated land; Non, none salinization; Mild, mild salinization; Mod, moderate salinization; Sev, severe salinization.

(35.33%), and severe (2.33%) salinization (Pillar 9 of Fig. 6). The grades of salinization of "increased cultivated land" are determined by many factors, e.g., the initial attributes of the land, management modes, and other factors. We further explore the impact of various influencing factors on soil salinization in the discussion section.

"Stable cultivated land" has an area of 20,563.01 km^2. After ten years of treatment, we observed that the proportion of mild, moderate, and severe salinization had decreased significantly (Pillar 11–12 of Fig. 6). Mild salinization decreased by 4.38% (30.08% in 2005 and 25.70% in 2014), moderate salinization dropped from 7.91% to 3.47%, and severe salinization was reduced from 0.12% to 0.06%. These results indicated that the treatment of soil salinization in stable cultivated land was very effective in the past ten years.

4. Discussion

4.1. Soil salinization in arid regions

This study aims to explore the potential impact o landscape dynamics on soil salinization. With the increasing trend of global warming, soil salinization in low and middle-latitude regions has become increasingly prominent (D'Odorico et al., 2013). Soil salinization in some countries (e.g., the United States, China, Hungary, and Australia) is becoming severe. In northern and eastern Africa, South America, the Middle East, Central Asia, and South Asia, soil salinization is expected to be worsened (Acosta et al., 2011), posing threats to agricultural development and food security as well as causing a variety of issues that include land desertification and land degradation (Muyen et al., 2011).

As discussed in the literature review session, many efforts have been made on the evaluation of soil salinization, and most of these studies choose arid regions as targets (Rath and Rousk, 2015). El Harti et al. (2016) proposed a new soil salinity index (OLI-SI) to monitor salinization in the Tadla plain in central Morocco by using spectral indices derived from Thematic Mapper (TM) and Operational Land Imager (OLI) data. Farzamian et al. (2019) used electromagnetic instruments to measure the soil apparent electrical conductivity (EC_a), which was then inverted to generate electromagnetic conductivity images, providing the vertical distribution of the soil electrical conductivity. Wang et al. (2020) established a comprehensive scoring system for evaluating the risk of salinity in the dry and wet seasons in the Ebinur Lake Wetland National Nature Reserve (ELWNNR). We argue that solely relying on remote sensing technology to quantitatively study soil salinization usually fails to achieve desired results. Approaches that integrate remote sensing technologies and ground measurements are preferred.

The northern slope of Tianshan Mountains is a typical arid zone, facing a serious threat of soil salinization. In this study, we established a new comprehensive method to evaluate soil salinization. According to the second Chinese national soil survey in 1985, the salinized cultivated land in Xinjiang Province accounted for 30.85% of the total cultivated land. This ratio is very close to the results of this study, which confirms, to a large extent, the credibility of the evaluation results. Taking the year 2014 as an example, salinized cultivated land covered an area of 7785.60 km^2, accounting for 32.11% of the cultivated land, a much higher value compared to the national average level (6.62%) in China (Tian et al., 2016; Zhang et al., 2020). Soil salinization was concentrated in the central sub-region (5,186.05 km^2, occupying 66.61% of the total area of soil salinization). The spatial distribution of soil salinization differs in arid and humid regions. For example, Yang et al. (2020) studied the spatiotemporal dynamics of soil salinization in Shandong Province from 1979 to 2016. They found the area of salinized cultivated land was 255.74 km^2, accounting for 11.30% of the cultivated land. Soil salinization showed a concentrated distribution along the coastal plain while scattered in the Yellow River flood plain and inland areas. Comparing the statistics, it is clear that soil salinization in arid regions is considerably severe than that in humid regions.

4.2. Mitigating soil salinization

Soil salinization mitigation has been a strategic goal for the sustainable development of irrigated agriculture and the improvement of environmental quality in arid regions (Akramkhanov et al., 2014). Major mitigation measures of salinization include water conservancy improvement (farmland drainage), agricultural improvement (drying ridges and backfilling of other soil), chemical improvement (various amendments), and biological improvement (salt-tolerant crops) (Bagheri et al., 2019). This study suggests that remote sensing images should be combined with ground surveys to build a regional spatial database of soil salinization. The agricultural department should

monitor soil salinization regularly by compiling salinization maps and establish an early risk assessment mechanism. With existing irrigation systems, biological and chemical measures should also be used to control soil salinization.

Without considering the dynamics in landscape, soil salinization cannot be estimated in a comprehensive and accurate manner (Gebremeskel et al., 2018a). In this study, we calculated the proportions of four soil salinization categories (i.e., severe, moderate, mild, and none) in the decreased, increased, and stable cultivated lands. The soil salinization in stable cultivated land can best reflect the effectiveness of treatment. The results indicated that the proportions of mild (from 30.08% to 25.70%), moderate (7.91–3.47%), and severe salinized cultivated land (0.12–0.06%) had decreased significantly during the study period (Fig. 6). We acknowledge that great improvement of soil salinization has been achieved in the past ten years. We need to continue the implementation of various mitigation measures while keep investigating the evolution of soil salinization under the background of landscape dynamics.

4.3. Implications for land resource management in arid regions

Numerous traditional studies have analyzed the heterogeneity of soil salinization in different landscape patterns (Chen et al., 2019; Khongnawang et al., 2020; Yang et al., 2019). However, few studies clarify the impact of landscape pattern changes on soil salinization. In this study, we found that changes in landscape patterns are responsible for the transformation of the grades of soil salinization (usually, this process is irreversible). Our results indicated that the proportion of soil salinization was only 13.96% (mild salinization occupying 8.72% and moderate salinization occupying 5.24%) in the decreased cultivated land. However, the proportion of salinized cultivated land reached 59.11% (mild salinization occupying 43.58%, moderate salinization occupying 13.51%, and severe salinization occupying 2.02%) in the increased cultivated land (Fig. 6). Obviously, the proportion of soil salinization in the increased cultivated land was much higher than that in decreased cultivated land. The proportion of soil salinization in stable cultivated land decreased by 8.89% (38.11% in 2005 and 29.22% in 2014).

The findings in our study provide enough evidence to prove: (1) improvement of soil salinization in stable cultivated land is effective; (2) most of the decreased cultivated land in the process of urbanization is high-quality cultivated land (cultivated land with an area of 604.79 km^2 was converted to construction land); (3) the increased cultivated land was a decisive factor for the increase in soil salinization. These findings provide scientific references for the improvement of soil salinization and the management of land resources in arid regions and are of great value for the food security and the sustainable development of irrigated agriculture in arid regions.

4.4. Limitations and prospects

We need to acknowledge some minor limitations. First, we combined remote sensing technology with ground measurement to evaluate the salinization level. However, the potential of intelligent statistical analysis should be explored. Second, the driving factors of soil salinization is still a complex and difficult task. Further studies need to acknowledge the multi-faceted nature of soil salinization and evaluate this problem from other perspectives.

Recent years have seen the rapid development of deep learning techniques. Numerous deep learning based estimation models of soil salinization have been established. Remote sensing technology and machine learning algorithms are expected to benefit large-scale soil salinization monitoring, providing a great opportunity for the development of intelligent irrigation.

5. Conclusion

Soil salinization, resulting from a combined effect of human factors and natural factors, poses a great threat to the sustainable development of the agricultural system and is responsible for declined crop productivity, land degradation, and reduced biodiversity. Contradiction exists between the growing demand for food and the inhibition of soil salinization on productivity. This study demonstrated that landscape changing dynamics have a great influence on soil salinization, providing important references for coordinating cultivated land resources and tackling the urgency of food security. The following conclusions were justified by the results of this study.

Firstly, we established a classification method for soil salinization based on AHP. We derived the spatial distribution of soil salinization in the two different phases (2005 and 2014) in the irrigated northern slopes of the Tianshan Mountains. Cultivated lands with soil accounted for a relatively high proportion of the total cultivated land area (28.21% in 2005 and 32.11% in 2014). One of the major contributions of this research lies in the detailed analysis of the spatiotemporal heterogeneity of soil salinization from three different types of cultivated lands, i.e., stable cultivated land, decreased cultivated land, and increased cultivated land. We found that the proportion of soil salinization decreased by 8.89% (38.11% in 2005 and 29.22% in 2014) in stable cultivated land. None salinization category was dominant in decreased cultivated land, occupying 86.05% of the total area of decreased cultivated land. The proportion of soil salinization in increased cultivated land was 59.11%, with mild, moderate, and severe salinization accounting for 43.58%, 13.51%, and 2.02%, respectively.

This study investigated the spatiotemporal characteristics of soil salinization under the background of landscape patterns in the irrigated northern slopes of the Tianshan Mountains, enriching the scientific connotation of the sustainable development of agriculture in arid regions. By linking the spatiotemporal landscape dynamics with soil salinization, we provided scientific evidence that potentially benefits local authorities and assists in tackling the severe food security issue in the study region.

Declaration of Competing Interest

The authors declare that they have no known competing financial interests or personal relationships that could have appeared to influence the work reported in this paper.

Acknowledgments

We would like to extend sincere gratitude to the academic editor and reviewers for their constructive comments which greatly helped us to improve the quality of this manuscript. is work is supported by the National Key Research and Development Program of China under Grant 2018YFB0505401, the Research Project from the Ministry of Natural Resources of China under Grant 4201–240100123, the National Natural Science Foundation of China under Grants 41771452, 41771454 and 41890820, the Natural Science Fund of Hubei Province in China under Grant 2018CFA007.

Appendix A. Supplementary material

Supplementary data to this article can be found online at https://doi.org/10.1016/j.catena.2021.105561.

References

Acosta, J.A., Jansen, B., Kalbitz, K., Faz, A., Martinez-Martinez, S., 2011. Salinity increases mobility of heavy metals in soils. Chemosphere 85 (8), 1318–1324.
Adejumobi, M.A., Awe, G.O., Abegunrin, T.P., Oyetunji, O.M., Kareem, T.S., 2016. Effect of irrigation on soil health: a case study of the Ikere irrigation project in Oyo State, southwest Nigeria. Environ. Monit. Assess. 188 (12), 696.

Akramkhanov, A., Brus, D.J., Walvoort, D.J.J., 2014. Geostatistical monitoring of soil salinity in Uzbekistan by repeated EMI surveys. Geoderma 213, 600–607.
Aly, Z., Bonn, F.J., Magagi, R., 2007. Analysis of the backscattering coefficient of salt-affected soils using modeling and RADARSAT-1 SAR data. IEEE Trans. Geosci. Remote Sens. 45 (2), 332–341.
Asiedu, E., Sadekla, S.S., Bokpin, G.A., 2020. Aid to Africa's agriculture towards building physical capital: Empirical evidence and implications for post-COVID-19 food insecurity. World Dev. Perspect. 20, 100269.
Bagheri, R., Nosrati, A., Jafari, H., Eggenkamp, H.G.M., Mozafari, M., 2019. Overexploitation hazards and salinization risks in crucial declining aquifers, chemo-isotopic approaches. J. Hazard. Mater. 369, 150–163.
Bai, K., Li, K., Chang, N.-B., Gao, W., 2019. Advancing the prediction accuracy of satellite-based PM2.5 concentration mapping: a perspective of data mining through in situ PM2.5 measurements. Environ. Pollut. 254, 113047.
Bless, A.E., Colin, F., Crabit, A., Devaux, N., Philippon, O., Follain, S., 2018. Landscape evolution and agricultural land salinization in coastal area: a conceptual model. Sci. Total Environ. 625, 647–656.
Bordonal, R.d.O., Lal, R., Ronquim, C.C., de Figueiredo, E.B., Nunes Carvalho, J.L., Maldonado, W., Jr., Bastos Pereira Milori, D.M., La Scala, N., Jr., 2017. Changes in quantity and quality of soil carbon due to the land-use conversion to sugarcane (Saccharum officinarum) plantation in southern Brazil. Agric. Ecosyst. Environ. 240, 54–65.
Chen, C., Park, T., Wang, X., Piao, S., Xu, B., Chaturvedi, R.K., Fuchs, R., Brovkin, V., Ciais, P., Fensholt, R., Tommervik, H., Bala, G., Zhu, Z., Nemani, R.R., Myneni, R.B., 2019. China and India lead in greening of the world through land-use management. Nat. Sustainability 2 (2), 122–129.
D'Odorico, P., Bhattachan, A., Davis, K.F., Ravi, S., Runyan, C.W., 2013. Global desertification: drivers and feedbacks. Adv. Water Resour. 51, 326–344.
Daliakopoulos, I.N., Tsanis, I.K., Koutroulis, A., Kourgialas, N.N., Varouchakis, E.A., Karatzas, G.P., Ritsema, C.J., 2016. The threat of soil salinity: a European scale review. Sci. Total Environ. 573, 727–739.
Dehaan, R.L., Taylor, G.R., 2002. Field-derived spectra of salinized soils and vegetation as indicators of irrigation-induced soil salinization. Remote Sensing of Environment 80(3), 406–417. Hydrogeol. J. 16, 281–296.
Druhan, J.L., Hogan, J.F., Eastoe, C.J., Hibbs, B.J., Hutchison, W.R., 2008. Hydrogeologic controls on groundwater recharge and salinization: a geochemical analysis of the northern Hueco Bolson aquifer, Texas, USA.
El Harti, A., Lhissou, R., Chokmani, K., Ouzemou, J.-E., Hassouna, M., Bachaoui, E.M., El Ghmari, A., 2016. Spatiotemporal monitoring of soil salinization in irrigated Tadla Plain (Morocco) using satellite spectral indices. Int. J. Appl. Earth Obs. Geoinf. 50, 64–73.
FAO, IFAD, UNICEF, WFP and WHO, 2020. The State of Food Security and Nutrition in the World 2020. Transforming food systems for affordable healthy diets. In: FAO, Rome. https://doi.org/10.4060/ca9692en.
Farzamian, M., Paz, M.C., Paz, A.M., Castanheira, N.L., Gonçalves, M.C., Monteiro Santos, F.A., Triantafilis, J., 2019. Mapping soil salinity using electromagnetic conductivity imaging—A comparison of regional and location-specific calibrations. Land Degrad. Dev. 30 (12), 1393–1406.
Funakawa, S., Suzuki, R., Karbozova, E., Kosaki, T., Ishida, N., 2000. Salt-affected soils under rice-based irrigation agriculture in southern Kazakhstan. Geoderma 97 (1–2), 61–85.
Gao, J., O'Neill, B.C., 2020. Mapping global urban land for the 21st century with data-driven simulations and Shared Socioeconomic Pathways. Nat. Commun. 11 (1), 2303.
Gebremeskel, G., Gebremicael, T.G., Hagos, H., Gebremedhin, T., Kifle, M., 2018a. Farmers' perception towards the challenges and determinant factors in the adoption of drip irrigation in the semi-arid areas of Tigray, Ethiopia. Sustainable Water Resour. Manage. 4 (3), 527–537.
Gebremeskel, G., Gebremicael, T.G., Kifle, M., Meresa, E., Gebremedhin, T., Girmay, A., 2018b. Salinization pattern and its spatial distribution in the irrigated agriculture of Northern Ethiopia: an integrated approach of quantitative and spatial analysis. Agric. Water Manag. 206, 147–157.
Hoffman, M.T., Skowno, A., Bell, W., Mashele, S., 2018. Long-term changes in land use, land cover and vegetation in the Karoo drylands of South Africa: implications for degradation monitoring(</n>). Afr. J. Range Forage Sci. 35 (3–4), 209–221.
Hong, J., Huang, W.P., Makino, T., 1993. Modeling of ridge-wave-guide mqw DFB lasers based on spectral index transfer-matrix method. IEEE J. Quantum Electron. 29 (6), 1743–1750.
Huq, M.E., Fahad, S., Shao, Z., Sarven, M.S., Al-Huqail, A.A., Siddiqui, M.H., Rahman, M. H.U., Khan, I.A., Alam, M., Saeed, M., Rauf, A., Basir, A., Jamal, Y., Khan, S.U., 2019. High arsenic contamination and presence of other trace metals in drinking water of Kushtia district, Bangladesh. J. Environ. Manage. 242, 199–209.
IGBP, 2005. cience Plan and Implementation Strategy. In: G. Secretariat, Stockholm, SWEDEN.
Islam, M.A., Hoque, M.A., Ahmed, K.M., Butler, A.P., 2019. Impact of Climate Change and Land Use on Groundwater Salinization in Southern Bangladesh-Implications for Other Asian Deltas. Environ Manage 64 (5), 640–649.
Jiang, H., Shu, H., 2019. Optical remote-sensing data based research on detecting soil salinity at different depth in an arid-area oasis, Xinjiang, China. Earth Sci. Inf. 12 (1), 43–56.
Jiang, L., Jiapaer, G., Bao, A., Kurban, A., Guo, H., Zheng, G., De Maeyer, P., 2019. Monitoring the long-term desertification process and assessing the relative roles of its drivers in Central Asia. Ecol. Ind. 104, 195–208.
Jordan, A., Zavala, L.M., Gil, J., 2010. Effects of mulching on soil physical properties and runoff under semi-arid conditions in southern Spain. Catena 81 (1), 77–85.
Kansiime, M.K., Tambo, J.A., Mugambi, I., Bundi, M., Kara, A., Owuor, C., 2021. COVID-19 implications on household income and food security in Kenya and Uganda: Findings from a rapid assessment. World Dev. 137, 105199–105199.
Khan, N.M., Rastoskuev, V.V., Sato, Y., Shiozawa, S., 2005. Assessment of hydrosaline land degradation by using a simple approach of remote sensing indicators. Agric. Water Manag. 77 (1–3), 96–109.
Khongnawang, T., Zare, E., Srihabun, P., Triantafilis, J., 2020. Comparing electromagnetic induction instruments to map soil salinity in two-dimensional cross-sections along the Kham-rean Canal using EM inversion software. Geoderma 377, 114611.
Kunst, F.K., Dwivedi, V., 2019. Non-Hermitian systems and topology: a transfer-matrix perspective. Physical Review B 99 (24), 245116.
Lakhdar, A., Rabhi, M., Ghnaya, T., Montemurro, F., Jedidi, N., Abdelly, C., 2009. Effectiveness of compost use in salt-affected soil. J. Hazard. Mater. 171 (1–3), 29–37.
Lambin E F, G.H.L., 2006. Land-use and land-cover change:Local processes and global impact. Springer, New York.
Li, J., Pu, L., Han, M., Zhu, M., Zhang, R., Xiang, Y., 2014. Soil salinization research in China: Advances and prospects. J. Geog. Sci. 24 (5), 943–960.
Li, P., Qian, H., Wu, J., 2018. Conjunctive use of groundwater and surface water to reduce soil salinization in the Yinchuan Plain, North-West China. Int. J. Water Resour. Dev. 34 (3), 337–353.
Liu, J., Zhang, Z., Zhang, S., Yan, C., Wu, S., Li, R., Kuang, W., Shi, W., Huang, L., Ning, J., Dong, J., 2020. Innovation and development of remote sensing-based land use change studies based on shupeng chen's academic thoughts. J. Geo-Inf. Sci. 22 (4), 680–687.
Muyen, Z., Moore, G.A., Wrigley, R.J., 2011. Soil salinity and sodicity effects of wastewater irrigation in South East Australia. Agric. Water Manag. 99 (1), 33–41.
Nativ, R., Adar, E., Dahan, O., Nissim, I., 1997. Water salinization in arid regions - Observations from the Negev desert, Israel. J. Hydrol. 196, 271–296.
Rath, K.M., Rousk, J., 2015. Salt effects on the soil microbial decomposer community and their role in organic carbon cycling: a review. Soil Biol. Biochem. 81, 108–123.
Shao, Z., Cai, J., Fu, P., Hu, L., Liu, T., 2019a. Deep learning-based fusion of Landsat-8 and Sentinel-2 images for a harmonized surface reflectance product. Remote Sens. Environ. 235, 111425.
Shao, Z., Li, C., Li, D., Altan, O., Zhang, L., Ding, L., 2020a. An accurate matching method for projecting vector data into surveillance video to monitor and protect cultivated land. ISPRS Int. J. Geo-Inf. 9 (7), 448.
Shao, Z., Wang, L., Wang, Z., Deng, J., 2019b. Remote sensing image super-resolution using sparse representation and coupled sparse autoencoder. IEEE J. Sel. Top. Appl. Earth Obs. Remote Sens. 12 (8), 2663–2674.
Shao, Z., Wu, W., Guo, S., 2020b. IHS-GTF: a fusion method for optical and synthetic aperture radar data. Remote Sensing 12 (17), 2796.
Smith, P., House, J.I., Bustamante, M., Sobocka, J., Harper, R., Pan, G., West, P.C., Clark, J.M., Adhya, T., Rumpel, C., Paustian, K., Kuikman, P., Cotrufo, M.F., Elliott, J.A., McDowell, R., Griffiths, R.I., Asakawa, S., Bondeau, A., Jain, A.K., Meersmans, J., Pugh, T.A.M., 2016. Global change pressures on soils from land use and management. Glob. Change Biol. 22 (3), 1008–1028.
Tang, W., Hu, J., Zhang, H., Wu, P., He, H., 2015. Kappa coefficient: a popular measure of rater agreement. Shanghai Arch. Psychiatry 27 (1), 62–67.
Tian, C., Mai, W., Zhao, Z., 2016. Study on key technologies of ecological management of saline alkali land in arid area of Xinjiang. Acta Ecol. Sin. 36 (22), 7064–7068.
Wang, S., Ju, W., Penuelas, J., Cescatti, A., Zhou, Y., Fu, Y., Huete, A., Liu, M., Zhang, Y., 2019. Urban-rural gradients reveal joint control of elevated CO2 and temperature on extended photosynthetic seasons. Nat. Ecol. Evol. 3 (7), 1076–1085.
Wang, Z., Zhang, F., Zhang, X., Chan, N.W., Kung, H.-T., Zhou, X., Wang, Y., 2020. Quantitative evaluation of spatial and temporal variation of soil salinization risk using GIS-based geostatistical method. Remote Sensing 12 (15), 2405.
Xiao, Y., Zhao, G., Li, T., Zhou, X., Li, J., 2019. Soil salinization of cultivated land in Shandong Province, China-Dynamics during the past 40 years. Land Degrad. Dev. 30 (4), 426–436.
Yang, C., Wang, X., Miao, F., Li, Z., Tang, W., Sun, J., 2020. Assessing the effect of soil salinization on soil microbial respiration and diversities under incubation conditions. Appl. Soil Ecol. 155, 103671.
Yang, X., Tsibart, A., Nam, H., Hur, J., El-Naggar, A., Tack, F.M.G., Wang, C.-H., Lee, Y. H., Tsang, D.C.W., Ok, Y.S., 2019. Effect of gasification biochar application on soil quality: Trace metal behavior, microbial community, and soil dissolved organic matter. J. Hazard. Mater. 365, 684–694.
Yaseen, Z.M., Al-Juboori, A.M., Beyaztas, U., Al-Ansari, N., Chau, K.-W., Qi, C., Ali, M., Salih, S.Q., Shahid, S., 2020. Prediction of evaporation in arid and semi-arid regions: a comparative study using different machine learning models. Eng. Appl. Comput. Fluid Mech. 14 (1), 70–89.
Zhang, R., Shao, Z., Huang, X., Wang, J., Li, D., 2020a. Object detection in UAV images via global density fused convolutional network. Remote Sensing 12, 3140.
Zhang, Z., Ding, J., Wang, J., Ge, X., Wang, J., Tian, M., Zhao, Q., 2020b. Digital Soil properties mapping by ensembling soil-environment relationship and machine learning in arid regions. Sci. Agric. Sin. 53 (3), 563–573.
Zhuang, Q., Wu, S., Yan, Y., Niu, Y., Yang, F., Xie, C., 2020. Monitoring land surface thermal environments under the background of landscape patterns in arid regions: A case study in Aksu river basin. Sci. Total Environ. 710, 136336.